Sub-shot-noise-limited fiber-optic quantum receiver

M. L. Shcherbatenko, M. S. Elezov, and G. N. Goltsman*
Moscow State Pedagogical University, 1/1 M. Pirogovskaya Street, Moscow 119992, Russia

D. V. Sych†
P. N. Lebedev Physical Institute, Russian Academy of Sciences, 53 Leninskiy Prospekt, Moscow 119991, Russia;
QRate, Novaya avenue 100, Moscow 121353, Russia;
and Moscow State Pedagogical University, 1/1 M. Pirogovskaya Street, Moscow 119992, Russia

(Received 20 December 2019; accepted 5 February 2020; published 5 March 2020)

We experimentally demonstrate a quantum receiver based on the Kennedy scheme for discrimination between two phase-modulated weak coherent states. The receiver is assembled entirely from standard fiber-optic elements and operates at a conventional telecom wavelength of 1.55 μm. The local oscillator and the signal are transmitted through different optical fibers, and the displaced signal is measured with a high-efficiency superconducting nanowire single-photon detector. We show the discrimination error rate is two times below that of a shot-noise-limited receiver with the same system detection efficiency.

DOI: 10.1103/PhysRevA.101.032306

I. INTRODUCTION

Since the beginning of telecommunications there has been an ever increasing demand to transmit more data. Optical signals are ideal carriers of information over long distances due to their high capacity and speed. An optical receiver has to convert the optical signal into logical data. An important performance index of different receivers is the error rate, i.e., the probability to transmit a single bit incorrectly. Quantum properties of light set the fundamental limits on the minimum error rate. With the use of Gaussian operations, the minimum error is bounded by the shot noise or the so-called standard quantum limit (SQL) [1]. The use of non-Gaussian operations (e.g., single-photon detectors) can reduce the error rate to a lower value, bounded from below by the Helstrom bound [2,3]. In theory, several types of quantum receivers may be used to overcome the SQL [4–15] or even approach the Helstrom bound for certain types of signals [16–19]. However, in practice, it is very difficult to experimentally demonstrate sub-SQL performance due to several reasons.

First, most theoretical proposals of sub-SQL receivers involve the optical displacement of the communication signal [i.e., interference of the signal with a reference light beam, called the local oscillator (LO)], followed by its measurement with the help of a single-photon detector (SPD). To realize stable and high-contrast interference, LO must be perfectly mode-matched to the signal. Moreover, in the first theoretical proposal of the quantum receiver that reaches the Helstrom bound (Dolinar receiver) [16], the phase and amplitude of LO must be dynamically adjusted depending on the output of the SPD via instantaneous feedback. A recently developed optimal multichannel quantum receiver [17] does not require instantaneous feedback, but involves several optical displacement operations. Another approach to reach the Helstrom bound involves the nonlinear transformation of the signal, which is extremely challenging to realize in practice [18].

Second, the overall system detection efficiency of the receiver, including the quantum efficiency of SPD, must be high—above 50% for the binary signal [2]. Apart from high quantum efficiency, the SPD must have a low dark count rate and short dead time, which is rather difficult to combine. Superconducting nanowire single-photon detectors (SNSPDs) [20] show great potential in this context, since they have a quantum efficiency close to 100%, the dead time is below 10 ns, and dark counts can be as low as 0.01 counts/s [21–24]. SNSPD is coupled with a single-mode fiber, which makes it relatively easy to integrate into a fiber-optic receiver scheme.

In this article we experimentally realize the simplest and historically the first sub-SQL receiver design, called a Kennedy receiver [4]. In order to meet the above-mentioned requirements for sub-SQL performance, we combine standard single-mode fiber-optic components to realize a high-extinction optical displacement operation and an SNSPD to detect the displaced signal. The receiver operates at a conventional telecommunication wavelength of 1.55 μm. We experimentally demonstrate that the maximal improvement of the error rate is about two times with respect to the SQL.

Note that previous experimental attempts towards sub-SQL quantum receivers, as well as quantum receivers aimed at other optimization strategies [25–27], were partially or fully implemented using optical components in free space. The use of standard fiber-optic components brings this area of research closer to real-world applications, since the vast majority of devices in classical optical communication use optical fiber technology. Compared to free-space optics, fiber-optic devices are more compact, reproducible, and convenient for practical use. It is easier to scale them up, which is important for the development of improved quantum receivers [17,19].

*goltsman@rplab.ru
†denis.sych@gmail.com

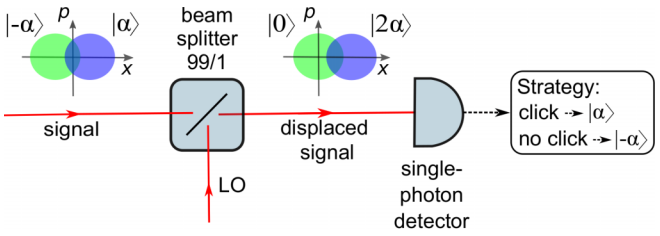

FIG. 1. Schematics of a displacement-based Kennedy receiver. A mode-matched signal and local oscillator are combined on a 99:1 beam splitter such that after the beam splitter one of the possible states (e.g., $|-\alpha\rangle$) vanishes out due to destructive interference with the local oscillator (LO). The result of interference between the signal and LO is registered by a single-photon detector.

II. KENNEDY RECEIVER

In the simplest form, the problem of minimum-error state discrimination is as follows. Consider the signal prepared in one of two equiprobable phase-modulated coherent states $|\alpha\rangle, |-\alpha\rangle$—the so-called binary phase-shift keyed (BPSK) signal. The main task of a receiver is to make some measurement of the signal and find out the actual signal state.

According to Kennedy's proposal [4], the measurement should be done by interfering the signal with a mode-matched reference beam (local oscillator, LO) on a beam splitter, such that after the beam splitter one of the possible states vanishes out due to destructive interference with the LO: $|\alpha\rangle, |-\alpha\rangle \rightarrow |2\alpha\rangle, |0\rangle$. To reduce the attenuation of the signal, interference is performed on an almost completely transparent beam splitter (99:1 splitting ratio) [28]. Such an operation is called exact nulling displacement. Afterwards, the displaced signal is measured with the help of a single-photon detector (see Fig. 1). If the detector gives a photocount ("click" event), then we can be sure that the signal was in the state which is not nulled (receive logical "1"), while in the case of no photocounts ("no-click" event), the most probable state is the nulled signal (receive logical "0").

The photon number distribution and the error diagram for the Kennedy receiver is shown in Fig. 2. Errors e_{01} of the ideal Kennedy receiver should be equal to zero, since a perfectly nulled signal gives no photocounts. Errors e_{10} come from the fact that "no-click" events may appear not only from the nulled signal $|0\rangle$, but also from the zero-photon component of the signal $|2\alpha\rangle$, i.e., nonzero signal is decoded incorrectly upon a "no-click" event. The probability distribution of n-photon components of the coherent state $|x\rangle$ is given by the Poisson distribution $P_n(x) = e^{-x^2}x^{-2n}/n!$, which is shown in Fig. 2. Thus the error rate of the Kennedy receiver is given by

$$e_K(m) = 0.5P_0(2\alpha) = 0.5e^{-4m}, \tag{1}$$

where $m = \alpha^2$ is the mean number of photons in the initial signal. For comparison, the error rate of the heterodyne receiver is given by [17]

$$e_{\mathrm{SQL}}(m) = \tfrac{1}{2}[1 - \mathrm{erf}(\sqrt{2m})], \tag{2}$$

where $\mathrm{erf}(x) = \frac{2}{\sqrt{\pi}}\int_0^x e^{-t^2}dt$, and the Helstrom bound is given by

$$e_{\mathrm{Hel}}(m) = \tfrac{1}{2}[1 - (\sqrt{1 - e^{-4m}})]. \tag{3}$$

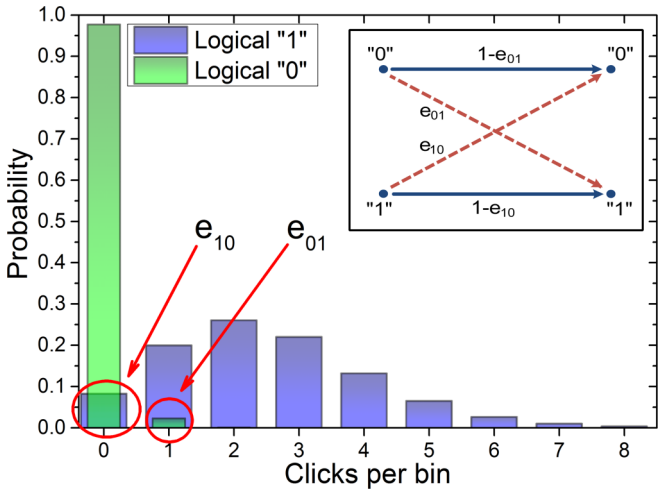

FIG. 2. Probability distribution of photocounts for logical "0" (green histogram), and logical "1" (blue histogram). Discrimination errors e_{10} and e_{01} correspond to the first component of the blue histogram (zero number of photocounts) and all-but-first components of the green histogram (nonzero number of photons), respectively. The inset shows the error diagram.

These values, normalized to SQL, are shown by the solid and dotted lines in Fig. 5.

To realize optical displacement, it is necessary to perform mode matching of the signal and LO. This means that all parameters describing the mode of the signal and the mode of the local oscillator must coincide. In the experiment it is difficult to achieve mode matching of the spatial, temporal, spectral, and polarization distributions for the light beams coming from different light sources. Thus technically both the LO and signal source are prepared by splitting one light source into two unequal parts: The larger part serves as the LO, and the smaller part is phase modulated and serves as the signal [6,9,14]. After mixing them on a properly balanced beam splitter, the mode-matching condition can be accomplished. In fact, this approach to the implementation of optical displacement resembles an unbalanced interferometer (for example, a Mach-Zehnder interferometer), in one of whose arms we prepare the signal, and in the second arm—the LO (see Fig. 3). To demonstrate experimentally a quantum receiver within this approach, it is necessary to ensure stabilization of the interferometer over all freedom degrees (polarization, phase, space, timing, etc.).

In reality, it is not possible to achieve perfect mode matching and perfect stabilization of the interferometer. First, due to the nonunit interference visibility, the state $|-\alpha\rangle$ is not completely nulled after the optical displacement. Second, nonzero dark counts contribute a certain level of background noise indistinguishable from nonperfect mode matching. As a result, a nonzero error e_{01} appears in the error diagram (see Fig. 2).

Using Eq. (2) in Ref. [17], the error rate of the Kennedy receiver accounting for the interference extinction $c = I_{\max}/I_{\min}$ (here, $I_{\max}$ and $I_{\min}$ are maximum and minimum intensities of the interference fringes) and dark counts dc (mean number of dark counts per signal bin) of the detector reads as

$$e'_K(m, c, dc) = 0.5e^{-4m} + 0.5(1 - e^{-dc-4m/c}), \tag{4}$$

which is shown by red dashed-dotted line in Fig. 5.

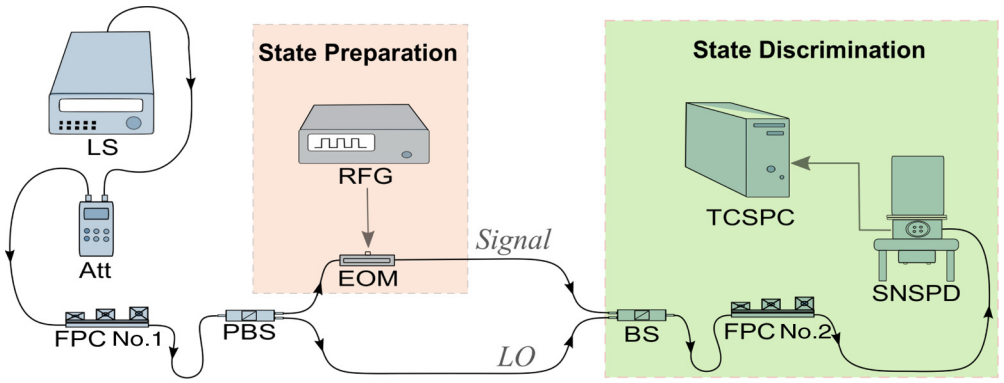

FIG. 3. Schematics of the experimental setup. The source of light (LS) is attenuated via a variable attenuator (ATT) and then split into two unequal parts on a polarization beam splitter (PBS). The splitting ratio is controlled by a fiber polarization controller (FPC No. 1). The two parts have the same polarization since one of the fibers is physically rotated by 90°. The weaker part is binary phase modulated on an electro-optical modulator (EOM) driven by a radio-frequency generator (RFG). The stronger part serves as a local oscillator that interferes with the signal on a beam splitter (BS). The result of interference is measured by a superconducting nanowire single-photon detector (SNSPD), preceded by a fiber polarization controller (FPC No. 2) to match the highest quantum efficiency of the detector. Time-correlated single-photon counting electronics (TCSPC) is used to synchronize the detector with the modulator.

To demonstrate the superiority of any Helstrom-bounded quantum receiver over the SQL, the minimum system detection efficiency η, including optical loss and detector quantum efficiency, should be such that $e_{\mathrm{Hel}}(\eta m) < e_{\mathrm{SQL}}(m)$, which implies $\eta \gtrsim 53\%$.

Minimum requirements for the Kennedy receiver to beat the SQL are even stronger: $e'_K(\eta m, c, dc) < e_{\mathrm{SQL}}(m)$. In this case, we have to comply with minimum system detection efficiency, minimum interference extinction, and maximum dark count rate. Provided noiseless detection ($dc = 0$) and perfect interference extinction ($c = \infty$), the minimum system detection efficiency must be $\eta \gtrsim 54\%$. The minimum interference extinction in the case of a unit system detection efficiency ($\eta = 1$) and noiseless detection ($dc = 0$) is $c \geqslant 80$. The maximum dark count rate, measured in photocounts per signal bin, in the case of a unit system detection efficiency ($\eta = 1$) and perfect interference extinction ($c = \infty$) is $dc = 0.035$.

It is quite possible to achieve each of these conditions separately. However, the realistic combination of all imperfections makes an experimental demonstration of the sub-SQL error rate rather challenging. For example, the real parameters of an experimental setup that we discuss in the next section are very good: The dark count rate is 300 Hz at a 200 kHz signal repetition rate ($dc = 0.0015$), and interference extinction is $c \simeq 1250$. To beat the SQL, the system detection efficiency should be such that $e'_K(\eta m, c = 1250, dc = 0.0015) < e_{\mathrm{SQL}}(m)$, which means $\eta \gtrsim 78\%$. The optical losses of beamsplitter connectors are around 0.3 dB ($\simeq 7\%$), thus the minimum quantum efficiency of the single-photon detector should be around 85%.

III. EXPERIMENTAL SETUP

Our experimental setup is shown in Fig. 3. We use the scheme based on the Mach-Zehnder interferometer, since it allows us to achieve high interference extinction and also has great potential for improving the receiver in the future. A highly coherent distributed-feedback (DFB) laser operating in the continuous-wave (cw) mode at a wavelength 1550 nm with linewidth 2 MHz is used as a light source. The power of the source is attenuated to the single-photon level by a tunable attenuator (Att). Light from the DFB laser is split by a polarization beam splitter (PBS). The splitting ratio is controlled by a mechanical polarization controller (FPC No. 1) to achieve the highest value of interference extinction. The second polarization controller (FPC No. 2) was used to adjust the polarization of the incident signal to the detector, as far as the quantum efficiency of SNSPD is polarization dependent.

To achieve maximum performance of the receiver, it is necessary to reduce some parasitic effects caused by optical fibers (such as polarization distortion, temperature fluctuations, vibrations, etc.) that influence the stability and contrast of the interferometer. To stabilize the optical scheme, the methods described in Refs. [29,30] were used. For polarization stability we use polarization-maintaining (PM) optical fiber components within the Mach-Zehnder interferometer. Phase stability is achieved by increasing the thermal inertia of the optical circuit. Optical fibers were thermally stabilized by a massive metal plate placed in a sealed box.

To estimate the discrimination error rate, it is necessary to compare the known signal at the receiver input with the decoded signal at the receiver output. Figure 4 illustrates the main steps we used to determine the error rate. An optical binary phase-modulated signal was generated using an electro-optical modulator (EOM). Signal parameters were controlled by a radio-frequency generator (RFG). The electrical signal has a meander shape with a repetition rate 100 kHz [see Fig. 4(a)]. We use this frequency since, on the one hand, it allows us to collect enough statistics of photocounts during the system stability time, and, on the other hand, it excludes the influence of the detector dead time (10 ns) on the statistics of photocounts. The voltage amplitude of EOM corresponds to the phase shift π. Then the signal is mixed with the LO (which has constant phase and power, matched to the signal power) that converts phase modulation into amplitude

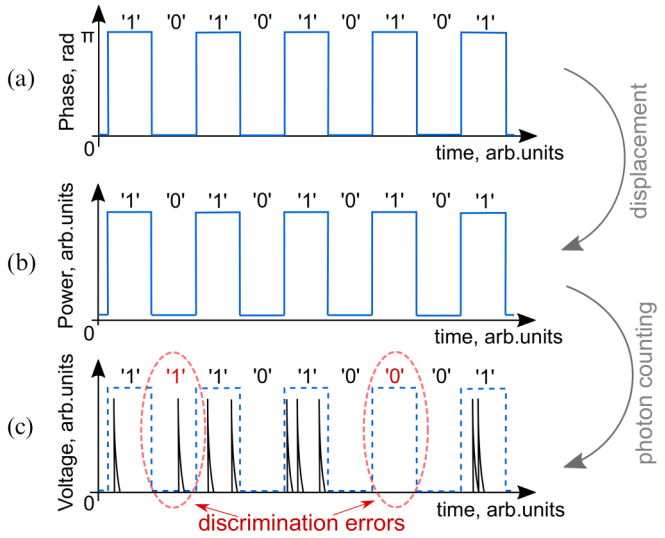

FIG. 4. Schematics of data processing. (a) Initial binary data are encoded into the binary phase-shifted coherent signal. (b) After optical displacement, the binary phase-shift signal is transformed into the binary amplitude-modulated signal with the amplitude modulation extinction around 30 dB. (c) Finally, an amplitude-modulated signal is registered by a single-photon detector. Photocounts (shown by the solid line) are decoded into logical data and matched with the original data (shown by the dashed line). After a comparison of encoded and decoded data, the discrimination errors are calculated.

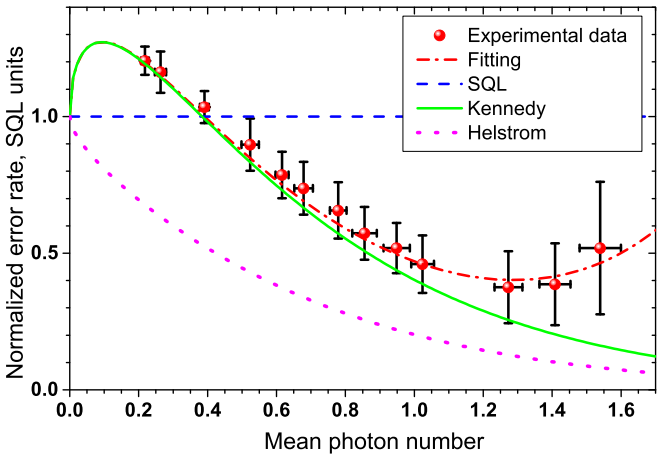

FIG. 5. Discrimination error rate as a function of mean photon number in a signal time bin. The error rate is normalized to the standard quantum limit (SQL), shown by the blue dashed line. Red dots show the experimental error rate of our receiver, including the statistical deviations indicated by black bars. The red dashed-dotted line shows a theoretical fit for the measured error rate. For comparison, we also show the theoretical values for the ideal Kennedy receiver (green solid line) and the Helstrom bound (magenta dotted line).

modulation [see Fig. 4(b)]. The displaced signal is detected by a single-photon detector which has 65% quantum efficiency, a dark count rate about 300 counts/s, and a dead time about 10 ns (SNSPD by SCONTEL) [31]. Detection events are recorded using time-correlated single-photon counting electronics (TCSPC) with a temporal resolution of 25 ps [see Fig. 4(c)]. The time intervals correspond to destructive interference encode logical "0," and constructive interference encode logical "1." The optimal selection of components for the passively stabilized optical scheme allows us to achieve an interference extinction of more than 30 dB ($I_{\max}/I_{\min} \simeq 1250$) for a time interval of several seconds. The data acquisition time is around 1 s.

By synchronizing the RFG signal generator, phase modulator controller, and TCSPC detection electronics, we can match the transmitted [Fig. 4(a)] and the received logical data [Fig. 4(c)] and determine the number of erroneously received bits. A bit is received erroneously if the half-period time window corresponding to a logical "0" contains some photocounts. This error e_{01} corresponds to the nonzero components of the green histogram (see Fig. 2). Also, a bit is received erroneously if the half-period time window corresponding to logical "1" contains no photocounts. This error e_{10} corresponds to the zero component of the blue histogram (see Fig. 2).

IV. EXPERIMENTAL RESULTS

Using experimental data, we calculate the error rate for different levels of signal intensities, measured in mean numbers of photons per signal time bin (or, simply, number of photons). The results are presented as red points in Fig. 5. All data points in Fig. 5 are normalized to the SQL [Eq. (2)].

Here, the mean photon number is derived from the mean number of photocounts without normalization to the system detection efficiency, i.e., we do not take into account optical losses (0.3 dB or 7% on the beam-splitter connectors, and 10% on the 90/10 beam splitter itself) and quantum efficiency of SNSPD (65%). As we discussed at the end of Sec. II, to demonstrate a truly sub-SQL performance, the minimum quantum efficiency that we need is substantially above 65%. In our case, we compare the Kennedy receiver with the shot-noise-limited system that has the same system efficiency ($0.65 \times 0.93 \times 0.9 \simeq 0.55$). The aim of this work is a proof-of-principle demonstration of an all-fiber Kennedy receiver. Technically, we could fuse two fibers and eliminate the optical loss of the beam-splitter connectors, as well as replace the beam splitter by a more asymmetric one (99/1) and the SNSPD by a more efficient one, available from SCONTEL, though in this work we do not do this.

For comparison, we show the Helstrom bound [Eq. (3)] by the magenta dotted line, the error rate of the ideal Kennedy receiver [Eq. (1)] by the green solid line, and the error rate of the nonperfect Kennedy receiver [Eq. (4)] by the red dashed-dotted line. The last curve fits well the experimental points for a dark count rate of ∼300 Hz, which corresponds to a dark count probability per signal bin $\sim 1.5 \times 10^{-3}$.

According to the obtained results, the Kennedy receiver has high sensitivity in the range between 0.5 and 1.6 photons. The experimentally observed error rate in this range is well below the SQL. The lowest error rate, normalized to SQL, was obtained for a signal intensity at 1.3 photons and is equal to 0.4 SQL.

For signal intensities at less than 0.4 photons, the performance of the Kennedy receiver is worse than SQL due to

the e_{10} error (the first component of the blue histogram in Fig. 2). This is the fundamental limitation of the Kennedy receiver. For signal intensities at higher than 1.6 photons, the performance of the Kennedy receiver is also worse than SQL, but this is a technical issue. In this case, the dominant contribution is e_{01} error (the nonzero components of the green histogram in Fig. 2). It originates from the nonunit interference visibility and dark counts, which set the background noise. The higher intensity of the signal, the larger is this contribution, and hence a higher discrimination error rate. To achieve high sensitivity of the receiver in this domain, we need to observe high interference extinction, which is a difficult task for practical implementation. Further progress in this direction may be associated with an improvement of the interference extinction, overall stability of the optical circuit, and development of novel receiver designs.

V. CONCLUSIONS AND OUTLOOK

We experimentally demonstrated an all-fiber quantum receiver based on Kennedy's design. We used a two-arm polarization-maintaining optical fiber Mach-Zehnder interferometer to create a binary phase-shift keyed signal in one arm and local oscillator in the other arm. Also, we used a very promising superconducting nanowire single-photon detector with excellent characteristics to measure the displaced signal. We achieved interference extinction above 30 dB, which allows us to observe a discrimination error rate below the SQL for a signal intensity level between 0.5 and 1.6 photons per time bin. The minimum value of the error rate that we experimentally obtain is 60% below the SQL on the condition that the signal is not normalized to the system detection efficiency.

The main motivation for this work is to demonstrate a quantum receiver solely based on standard fiber-optic components. The use of an optical fiber circuit makes it easier to employ the receiver in practical systems, such as quantum key distribution with discrete modulation of coherent states [32]. Our work is also aimed at creating a receiver with the potential for its further modernization and development of more advanced schemes [17]. We hope that the practical implementation of quantum receivers with high sensitivity can motivate their wider use in related research fields.

ACKNOWLEDGMENTS

We thank Scontel for providing a single-photon detector. The research has been carried out with the support of the Russian Science Foundation (Project No. 17-72-30036).

[1] J. A. Bergou, J. Mod. Opt. **57**, 160 (2010).
[2] C. W. Helstrom, Inf. Control **10**, 254 (1967).
[3] P. A. Bakut and S. S. Shchurov, Probl. Inf. Transm. (Engl. Transl.). **4**, 61 (1968).
[4] R. S. Kennedy, MIT RLE Quarterly Progress Report, Technical Report No. 108, 1973, pp. 219–225 (unpublished).
[5] F. E. Becerra, J. Fan, G. Baumgartner, S. V. Polyakov, J. Goldhar, J. T. Kosloski, and A. Migdall, Phys. Rev. A **84**, 062324 (2011).
[6] F. E. Becerra, J. Fan, G. Baumgartner, J. Goldhar, J. T. Kosloski, and A. Migdall, Nat. Photonics **7**, 147 (2013).
[7] R. S. Bondurant, Opt. Lett. **18**, 1896 (1993).
[8] C. R. Müller and C. Marquardt, New J. Phys. **17**, 032003 (2015).
[9] K. Tsujino, D. Fukuda, G. Fujii, S. Inoue, M. Fujiwara, M. Takeoka, and M. Sasaki, Phys. Rev. Lett. **106**, 250503 (2011).
[10] K. Tsujino, D. Fukuda, G. Fujii, S. Inoue, M. Fujiwara, M. Takeoka, and M. Sasaki, Opt. Express **18**, 8107 (2010).
[11] J. Chen, J. L. Habif, Z. Dutton, R. Lazarus, and S. Guha, Nat. Photonics **6**, 374 (2012).
[12] C. Wittmann, M. Takeoka, K. N. Cassemiro, M. Sasaki, G. Leuchs, and U. L. Andersen, Phys. Rev. Lett. **101**, 210501 (2008).
[13] M. Takeoka and M. Sasaki, Phys. Rev. A **78**, 022320 (2008).
[14] S. Guha, J. L. Habif, and M. Takeoka, J. Mod. Opt. **58**, 257 (2011).
[15] M. T. DiMario, L. Kunz, K. Banaszek, and F. E. Becerra, npj Quantum Inf. **5**, 65 (2019).
[16] S. Dolinar, MIT RLE Quarterly Progress Report, Technical Report No. 111, 1973, p. 115 (unpublished).
[17] D. Sych and G. Leuchs, Phys. Rev. Lett. **117**, 200501 (2016).
[18] M. Sasaki and O. Hirota, Phys. Rev. A **54**, 2728 (1996).
[19] M. Takeoka, M. Sasaki, P. van Loock, and N. Lütkenhaus, Phys. Rev. A **71**, 022318 (2005).
[20] G. Goltsman, O. Okunev, G. Chulkova, A. Lipatov, A. Semenov, K. Smirnov, B. Voronov, A. Dzardanov, C. Williams, and R. Sobolewski, Appl. Phys. Lett. **79**, 705 (2001).
[21] K. Smirnov, A. Divochiy, Y. Vakhtomin, P. Morozov, P. Zolotov, A. Antipov, and V. Seleznev, Supercond. Sci. Technol. **31**, 035011 (2018).
[22] K. Smirnov, Y. Vachtomin, A. Divochiy, A. Antipov, and G. Goltsman, Appl. Phys. Express **8**, 022501 (2015).
[23] F. Marsili, V. B. Verma, J. A. Stern, S. Harrington, A. E. Lita, T. Gerrits, I. Vayshenker, B. Baek, M. D. Shaw, R. P. Mirin, and S. W. Nam, Nat. Photonics **7**, 210 (2013).
[24] C. Natarajan, M. Tanner, and R. Hadfield, Supercond. Sci. Technol. **25**, 063001 (2012).
[25] C. Wittmann, U. L. Andersen, M. Takeoka, D. Sych, and G. Leuchs, Phys. Rev. Lett. **104**, 100505 (2010).
[26] C. Wittmann, U. L. Andersen, M. Takeoka, D. Sych, and G. Leuchs, Phys. Rev. A **81**, 062338 (2010).
[27] S. Izumi, M. Takeoka, K. Wakui, M. Fujiwara, K. Ema, and M. Sasaki, Phys. Rev. A **94**, 033842 (2016).
[28] S. Wallentowitz and W. Vogel, Phys. Rev. A **53**, 4528 (1996).
[29] M. Elezov, M. Scherbatenko, D. Sych, and G. Goltsman, J. Phys.: Conf. Ser. **1124**, 051014 (2018).
[30] M. Elezov, M. Scherbatenko, D. Sych, and G. Goltsman, EPJ Web Conf. **220**, 03011 (2019).
[31] http://www.scontel.ru.
[32] D. Sych and G. Leuchs, New J. Phys. **12**, 053019 (2010).